Accepted Manuscript

Porewater chemistry in compacted bentonite: Application to the engineered buffer barrier at the Olkiluoto site

Paul Wersin, Mirjam Kiczka, Kari Koskinen

PII: S0883-2927(16)30337-7

DOI: 10.1016/j.apgeochem.2016.09.010

Reference: AG 3721

To appear in: *Applied Geochemistry*

Received Date: 7 April 2016

Revised Date: 3 August 2016

Accepted Date: 23 September 2016

Please cite this article as: Wersin, P., Kiczka, M., Koskinen, K., Porewater chemistry in compacted bentonite: Application to the engineered buffer barrier at the Olkiluoto site, *Applied Geochemistry* (2016), doi: 10.1016/j.apgeochem.2016.09.010.

Porewater chemistry in compacted bentonite: application to the engineered buffer barrier at the Olkiluoto site

Paul Wersin[1*], Mirjam Kiczka[2], Kari Koskinen[3]

[1] University of Bern, Institute of Geological Sciences, Baltzerstrasse 1+3, 3012 Bern, Switzerland, paul.wersin@geo.unibe.ch

[2] Gruner Ltd, Gellertstrasse 55, 4020 Basel, Switzerland, mirjam.kiczka@gruner.ch

[3] Posiva Oy, Olkiluoto, 27160 Eurajoki, Finland, kari.koskinen@posiva.fi

Abstract

Compacted bentonite is used as sealing and buffer material in engineered barrier systems (EBS) of high-level radioactive waste repositories. The chemical characteristics of this clay and its porewater affect the migration of radionuclides eventually released from the waste. They also determine the integrity and long-term performance of the clay barriers. Key features are the structural negative charge and the large proportion of structural (interlayer) water of the main mineral montmorillonite, which leads to exclusion of anions and a surplus of cations in a large part of the porosity space. The objective of this contribution was to assess the impact of different porosity model concepts on porewater chemistry in compacted bentonite in the context of the planned Finnish spent nuclear fuel repository at Olkiluoto. First, a structural model based on well-established crystallographic and electrostatic considerations was set up to estimate the fractions of the different porosity types. In view of the uncertainty related to the chemical properties of the interlayer water, two very different model concepts (anion-free interlayer, Donnan space), together with a well-established thermodynamic model for bentonite, were applied to derive the porewater composition of the bentonite buffer at Olkiluoto. The simulations indicate very similar results in the "free" water composition for the two models and thus support the validity of the reference porewater concept commonly used in performance assessment of waste repositories. Differences between the models are evident in the composition of the water affected by the surface charge (i.e. diffuse double layer and interlayer). These reflect the conceptual uncertainty in current multi-porosity diffusion models.

Contents

*Corresponding author

Keywords: bentonite, porewater chemistry, modelling, engineered barrier system, nuclear waste repository

1. Introduction

Bentonite is used for many industrial and household applications. Owing to its plasticity, low permeability and swelling capacity compacted bentonite is also used as seal, backfill and buffer for nuclear waste repositories (Nagra 2002; Andra 2005; SKB 2011; Posiva 2013a). The main transport process in this clay material is diffusion and therefore the movement of contaminants eventually released from the waste is slow. The migration of many radionuclides and other solutes is affected by the porewater chemistry in the bentonite which regulates their sorption and precipitation behaviour (Ochs et al. 2004; Altmann 2008). In addition, the porewater chemistry in bentonite is an important starting point to evaluate the impact of other components in the repository (e.g. cement, steel) on the long term behaviour and performance of the buffer barrier (Posiva 2013a). The knowledge of the porewater chemistry in this material, however, is still incomplete. This is related to the nanoporous structure and the intimate clay-water association, which makes direct analysis of porewaters difficult and may lead to alteration in porewater chemistry during the sampling and/or analytical procedure (Sacchi et al. 2000).

A common approach to estimate the porewater composition in compacted bentonite has been thermodynamic modelling (Wieland et al. 1994; Bruno et al. 1999; Curti & Wersin 2002; Bradbury & Baeyens 2003; Wersin 2003; Wersin et al. 2004; Arcos et al. 2006), based on experimental data obtained at low clay/water ratios (Snellman et al. 1987; Wanner et al. 1994; Ohe & Tsukamoto 1997; Cuevas et al. 1997; Baeyens & Bradbury 1997; Muurinen & Lehikoinen 1999; Bradbury & Baeyens 2002). For example, Curti & Wersin (2002) could adequately describe the experimental data at different clay/water ratios (0.015-1.5 kg/L) from Muurinen & Lehikoinen (1999) with a simple thermodynamic model. This model considers reactions at the clay surface including cation exchange occurring at interlayer sites and pH-dependent protonation/deprotonation occurring at edge sites. Moreover, equilibrium reactions with accessory minerals in the bentonite, such as gypsum, calcite, quartz and kaolinite are included in the model. The modelling approaches in the studies mentioned above were based on similar thermodynamic concepts.

An inherent uncertainty in these models is the extrapolation of the thermodynamic model validated at low compaction degree to the compacted bentonite used for example as part of the engineered barrier system for high-level radioactive waste repositories (Wersin 2003; Bradbury & Baeyens 2003). In particular, the validity of electrostatic surface models (Tournassat et al. 2013) and the treatment of interlayer water (Wersin et al. 2004; Wersin et al. 2014a) have been questioned. Some valuable information in this regard has been obtained from experimental diffusion data. These data point to lower accessible porosities for anions as compared to neutral species and cations (Kozaki et al. 2001; Molera et al. 2003, Muurinen et al. 2007; Van Loon et al. 2007; Glaus et al. 2010). Based upon these findings, anion-exclusion models have been formulated, which subdivide the water-filled pore space into interlayer, diffuse (or electric) double layer (DDL) and “free” water porosities (Wersin et al. 2004; Tournassat & Appelo 2011; Appelo 2013). In this formulation, anions are considered to reside in the “free” electrically neutral solution and in the DDL in the external (intergranular) pores, whereas the interlayer (intragranular) space is considered devoid of anions. Support for this model has been given by molecular dynamics simulations (Rotenberg et al. 2007), but this issue remains controversial (Birgersson

& Karnland 2009). Birgersson & Karnland (2009) postulated an osmotic model in which the entire porespace is considered as Donnan space where both cations and anions reside. More recently, a double porosity model including DDL and free water has been applied for describing simultaneous cation and anion transport in bentonites (Alt-Epping et al. 2014; Tournassat & Steefel 2015). In this model type, no difference is made between the interlayer and the external diffuse double layer and anions can reside in this DDL space being only partially excluded by the negatively charged surface.

The general objective of this paper was to evaluate the different electrostatic and structural model concepts for compacted bentonite and their effect on porewater chemistry. A further objective was to test the robustness of porewater chemistry models for the bentonite buffer in the planned repository site for spent fuel at Olkiluoto, Finland . In a first step, the geochemical model with two cases was set up, based upon a well-established thermodynamic model approach (Wersin 2003; Curti & Wersin 2002; Wersin et al. 2004) and more recent microstructural and electrostatic concepts (Tournassat & Appelo 2011; Tournassat & Steefel 2015). Second, the model was applied to the Olkiluoto site by considering six different scenarios. Third, the results were compared and uncertainties highlighted in the light of the performance of the bentonite barrier in geological repositories.

2. Model description

2.1 Structural model

Bentonite used as buffer material in geological repositories consists at least of 75% of montmorillonite and accessory minerals, such as for example quartz, feldspar, illite, kaolinite, calcite and gypsum (Bradbury et al. 2014; SKB 2011; Posiva 2013a). The micro/nano structure of bentonite is largely determined by that of montmorillonite which may incorporate variable amounts of water in its interlayer (IL), depending on the nature of the interlayer cation, the layer charge induced by isomorphic substitution, ionic strength of the contacting solution, and montmorillonite mass per volume of water (Tournassat & Appelo 2011). At the outer surfaces, an electric or diffuse double layer (DDL) develops between the clay/water interface and the electrically neutral – “free” solution. Using these concepts the porosity of saturated bentonite is thus represented by three water types IL, DDL and “free” as schematically depicted in Fig. 1.

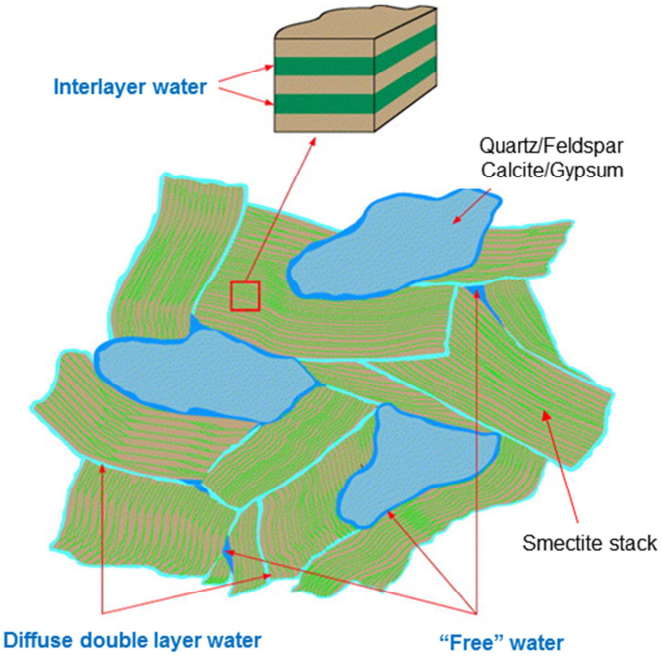

Fig. 1: Conceptual view of bentonite micro/nano structure and its porosity (modified from Bradbury & Baeyens 2003)

The relative proportions of the water types depend on various factors as outlined below, but because of uncertainties in microstructure and electrochemical properties vastly different models for porewater chemistry and solute diffusion have been proposed.

<u>TOT layer and interlayer porosity:</u>

The montmorillonite flakes are composed of negatively charged TOT layers alternating with 1-3 water layers containing charge compensating exchangeable cations (interlayers). The internal (basal) surface area of montmorillonite A_{int} (m^2/kg) can be calculated from the unit cell dimensions and the stacking number of TOT layers (Tournassat & Appelo 2011; Appelo 2013):

$$A_{\text{int}} = 2\frac{a \cdot b \cdot (n_c - 1)}{n_c}\frac{N_A}{MW}\ (\text{m}^2/\text{g}) \qquad (1)$$

where a (0.523 nm) and b (0.905 nm) are the unit lengths for montonclinic montmorillonite unit cell perpendicular to the c-axis, n_c is the stacking number in c direction, MW is the molecular weight of the montmorillonite and N_A is Avogadro's number ($6.022 \cdot 10^{23}$). The stacking number of TOT layers n_c in direction of the c axis depends on the type of interlayer cation (Pusch 2001, Melkior et al. 2009) and more generally on the prepraration and experimental conditions (Muurinen et al. 2007,Tournassat & Appelo 2011), as discussed below. The molecular weight of montmorillonite purified from MX-80 bentonite with the derived formula of $Na_{0.6}[Si_{7.92}Al_{0.08}][Al_{3.10}Mg_{0.48}Fe^{III}_{0.4}Fe^{II}_{0.02}]O_{20}OH_4$ (Madsen 1998) is 745.2 g/mol, which is similar to the MW (745.4 g/mol) derived by Kiviranta & Kumpulainen (2011). Assuming that the edge surface area is small compared to the total surface area, the total specific surface area of montmorillonte (ssm) can be approximated to:

135 $$ssm = 2a \cdot b \cdot \frac{N_A}{MW} (m^2/g) \quad (2)$$

136 The derived value from the crystallographic parameters and the molecular mass of montmorillonite is
137 765 m^2/g which is similar to that obtained by Madsen (1998) (749 m^2/g).

138 The interlayer porosity in bentonite depends on the expansion of montmorillonite in contact with
139 water. This expansion in turns depends on the exchangeable cation, the ionic strength, the bentonite's
140 density, and density of the interlayer water. Based upon leaching and squeezing data, Muurinen et al.
141 (2007) proposed for Na-rich MX-80 bentonite a simple relationship between interlayer distance (h_{IL}) and
142 bentonite dry density (ρ_{dry}): $h_{IL} = 1.41 \cdot 10^{-9} - 4.9 \cdot 10^{-13} \cdot \rho_d$, thus ignoring the effect of ionic strength. Later,
143 Tournassat & Appelo (2011) derived the relation for Na-montmorillonite for the transition of 3 layer
144 hydrate to two layer hydrate, following Bourg et al. (2006) and using XRD data from Kozaki et al. (1998,
145 2008):

146 $$h_{IL} = x_2 h_{IL}^{2WL} + x_3 h_{IL}^{3WL} \quad (3)$$

147 where x_2 and x_3 are the fractions of 2 layer hydrate and 3 layer hydrate, respectively with x2+x3=1. The
148 parameters h_{IL}^{2WL} (0.62 nm) and h_{IL}^{3WL} (0.94 nm) are the thicknesses of these hydrate layers. The fraction
149 x_2 varies between the montmorillonite dry density 1.3 kg/dm^3 (minimum) and 1.6 kg/dm^3 (maximum)
150 according to:

151 $$x_2 = \frac{\rho_{d,m} - (1.3 - 3c_{free})}{1.6 - (1.3 - 3c_{free})} \quad (4)$$

152 where $\rho_{d,m}$ is the montmorillonite dry density in kg/dm^3 and c is the concentration of NaCl in the "free"
153 external solution.

154 From the internal surface area A_{int} (m^2/g) and the h_{IL}, the interlayer porosity in a compacted bentonite
155 can be calculated:

156 $$\varepsilon_{IL} = \frac{A_{int}}{2} \cdot h_{IL} \cdot f_d \cdot w_{mm} \cdot \rho_d \quad (5)$$

157 where f_d is the density ratio of water in the interlayer and in the external pores and w_{mm} is the mass
158 fraction of montmorillonite. Assuming the same density of interlayer and external water (f_d=1)
159 (Tournassat & Appelo 2011) the interlayer porosity can be calculated from eqs. (2), (3) and (4).

160 Thus, the interlayer porosity is dependent on the bentonite density, the montmorillonite fraction, the
161 layer stacking number and the ionic strength. Application of eq. (5) shows that the amount of interlayer
162 porosity increases strongly with density and becomes a major porosity fraction above a density of 1.5
163 kg/dm^3. Considering the buffer target dry density 1.57 kg/dm^3 and a montmorillonite mass fraction of
164 0.75 in the Finnish concept (Posiva 2013a), then application of eq. (5) shows for a stacking number of 5
165 an interlayer porosity of 0.25 which is 53% of the total porosity. With a stacking number of 25 an
166 interlayer porosity of 0.29 is obtained corresponding to 62% of the total porosity. Note that at this
167 density the effect of ionic strength on interlayer porosity is small (within 1%).

168 <u>Diffuse double layer (DDL) and " free" water porosities:</u>

The external surface in montmorillonite consisting of basal and edge surfaces is influenced by the geometric configuration, thus the size and stacking number of the flakes. The average diameter of montmorillonite flakes is about 50 –200 nm (Pusch 2001, Plaschke et al. 2001, Tournassat et al. 2003, Le Forestier et al. 2010), leading to a stacking number of about 200 in the a and b directions (Tournassat & Appelo 2011; Appelo 2013). Under these premisses, the contribution of the edges to the external surface (A_{ext}) can be neglected and:

$$A_{ext} = 2\frac{a \cdot b}{n_c}\frac{N_A}{MW} = \frac{ssm}{n_c}\ (m^2/g) \qquad (6)$$

The negatively charged surface is compensated by an excess of cations in the diffuse layer. The concentrations in the DDL contacting a "free" electrically neutral solution can be obtained from formulations based on the Poisson-Boltzmann equation. For example, the concentrations in the diffuse layer can be calculated by the method of Borkovec & Westall (1983), which explicitly integrates the Poisson-Boltzmann equation (e.g. Wersin et al. 2004). Alternatively, the ions in the DDL can be averaged by considering the Donnan approximation (Leroy et al. 2006; Appelo & Wersin 2007; Tournassat & Appelo 2011), as outlined below. The thickness of the DDL is commonly expressed by the Debye length (d_{DDL}) (Appelo 2013):

$$d_{DDL} = \frac{3.09 \cdot 10^{-10}}{\sqrt{I}} f_{DDL}\ (m) \qquad (7)$$

where I is the ionic strength in the external pores and f_{DDL} is the number of Debye-lengths. The d_{DDL} has been shown to be difficult to constrain from experimental data in compact clays and f_{DDL} is often used as fitting parameter (Tournassat & Appelo 2011, Appelo 2013).

From the external surface area and the DDL thickness, the DDL porosity then becomes:

$$\varepsilon_{DDL} = A_{ext} \cdot d_{DDL} \cdot w_{mm} \cdot \rho_d \qquad (8)$$

The remaining porosity of the "free" solution is:

$$\varepsilon_{free} = \varepsilon_{tot} - \varepsilon_{IL} - \varepsilon_{DDL} \qquad (9)$$

Thus, from above equations the different porosity fractions for a given ionic strength can be derived if the stacking number n_c and the Debye length multiplier can be estimated. It is instructive to estimate the proportions of the different porosities for the bentonite buffer conditions and notably to evaluate the fraction of ε_{DDL} under different assumptions regarding n_c and f_{DLL}. The dependence of IL and DDL porosities as function of ionic strength for a bentonite dry density of 1.56 kg/dm^3 and w_{mm}= 0.75 is shown in Fig. 2. As pointed out above, the interlayer porosity shows only a very slight dependence on ionic strength and makes up about 52% and 62% of the total porosity for stacking numbers of 5 and 25, respectively. The effect of stacking number is much larger on the external DDL porosity. At low stacking number, thus high external surface area, the DDL porosity calculated from eq. (8) increases beyond the total porosity at lower ionic strength. This physically impossible result highlights the space constraints in the external pores of the compacted clay whose average thickness is in the same range as that of the interlayer. It also may suggest that a higher stacking number and thus a lower external surface area in the compacted clay should be considered. Support for a lower external surface in bentonite is provided

by BET measurements (Bradbury & Baeyens 2002) indicating an external surface area of ~30 m^2/g. This value corresponds to a stacking number of ~25 in our simple structural model. On the other hand, HRTEM measurements on compacted MX-80 bentonite samples (Melkior et a. 2009) indicate somewhat lower numbers of TOT layers, ranging from 1-10 for Na-bentonite, 7-50 layers for Ca-bentonite and for ~15 layers for a bentonite contacted with a mixed electrolyte solution. Referring again to our simple structural model, lower stacking numbers with high external surface areas at lower ionic strength would imply 1-2 Debye lengths (Fig. 2). At ionic strengths below 0.1 mol/L, this would imply a Debye-length below 1, meaning that the DDL would be overlapping.

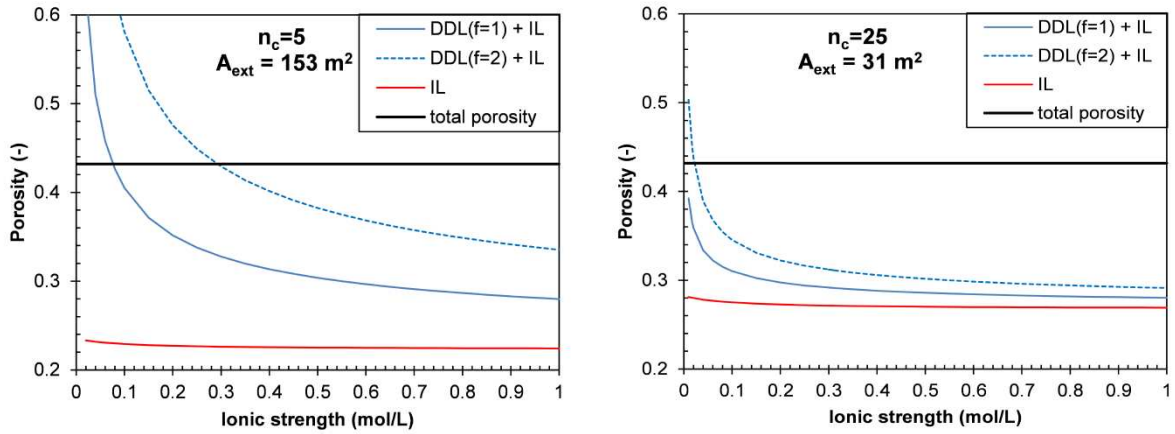

Fig. 2: Distribution of interlayer (IL) and diffuse double layer (DDL) porosity as function of ionic strength for different stacking numbers (n_c) and corresponding external surfaces areas (A_{ext}). Left: stacking number of 5. Right: stacking number of 25. Blue lines: sum of IL and DDL porosity with Debye length multiplier f = 1 (solid) and f = 2 (dashed). Red line: IL porosity.

From the above considerations, it appears that there are principally two parameters affecting the porosity distribution, which cannot be directly assessed, namely the stacking number n_c and the number of Debye lengths f_{DDL}. As discussed in Tournassat & Appelo (2011), diffusion data (see below) may help to bound the non-measurable parameters.

2.2 Estimates of model parameters based on diffusion data

There are different diffusion models for compacted bentonite, most of which, however are based upon the anion-exclusion and multi-porosity considerations (e.g. Leroy et al. 2006; Muurinen et al. 2007; Melkior et al. 2009; Tournassat & Appelo 2011; Alt-Epping et al. 2014). We also note the "single porosity" model of Birgersson & Karnland (2009) in which the entire porosity is lumped into one Donnan space. This latter model has been tested for simple NaCl electrolyte systems and, as discussed in Tournassat & Appelo (2011), appears to describe diffusion data adequately for a small range of bentonite densities, the details of which are not further discussed here.

Anion-free interlayer (AFI) models:

In these model types, the interlayer is considered to be devoid of anions and part of the crystallographic montmorillonite structure. Nevertheless, exchangeable cations may diffuse in this interlayer space as demonstrated by experimental data (e.g. Glaus et al. 2013).

Muurinen et al. (2007) equilibrated MX-80 bentonite samples at different densities (0.5 –1.5 kg/dm^3) with different NaCl solutions. They could adequately describe their chloride distribution by a double

porosity model including an anion-free interlayer and Donnan equilibrium between the external porosity and the external solution. An important parameter in their model was the external surface area which was taken to be either 20m^2/g for all densities or varied from 15-140 m^2/g from high to low densities.

Using anion-accessible porosity data of Muurinen (2006), Wersin et al. (2014a) conducted a preliminary fitting exercise based on an anion-free interlayer model described in Appelo (2013). Thereof, a stacking number of 4.8, a Debye length multiplier of 5.0 and an internal surface area of 487 m^2/g were estimated.

A systematic evaluation of anion-accessible porosity data (Muurinen et al. 1989; 2004; 2007; Molera et al. 2003; Van Loon et al. 2007) was done by Tournassat & Appelo (2011).The large scatter in the data was highlighted, likely explained by different composition and preparation of samples as well as the measurement procedure. Nevertheless, fairly good agreement between experimental and modelled anion-accessible porosities could be obtained in the range of 0.1–0.4 M ionic strengths. Different models with different assumptions and parameter variation were tested. In general, best fits were obtained by varying the stacking number as function of density and reducing the interlayer space to one water layer at high densities. The authors explained their model result by changes in the microstructure as function of compaction and ionic strength.

Donnan space (DS) models:

In these models, the interlayer porosity and external DDL porosity are considered as single Donnan space (also termed microporosity) which is in osmotic equilibrium with "free" water (also termed macroporosity) (Alt-Epping et al. 2014; Tournassat & Steefel 2015). This assumption is equivalent to an assumed stacking number of 1. The negatively charged surface is compensated by a surplus of cations in this space according to the Donnan approximation in which the surface potentials and ion concentrations in the DDL are averaged according to:

$$c_{D,i} = c_{free,i} \exp\left(\frac{-z_i F \psi_D}{RT}\right) \text{(mol/L)} \qquad (10)$$

where $C_{D,i}$ and $c_{free,i}$ is the concentration of species i in the Donnan space and the "free" solution, respectively, z_i is the charge of species i, and ψ_D is the Donnan potential. Note that a common approximation inherent in eq. (10) is to assume equal activity coefficients of the individual species in $C_{free,i}$ and $C_{D,I}$ which may not be the case (Appelo & Wersin 2007, Tournassat & Steefel 2015). The sum of ions in the Donnan space counterbalances the surface charge (q):

$$\sum_i z_i c_{D,i} + q = 0 \text{ (mol/L)} \qquad (11)$$

Thus, the Donnan potential is calculated from the condition imposed by eq. (11).

An advantage of DS models over AFI models (i.e. differentiating between an anion-free IL and an external DDL) is the fewer number of structural parameters required. For example, the porosity fraction of the Donnan space can be derived from double layer thickness according to eq. (7) and the total surface area of montmorillonite (Steefel et al. 2014). Due to the fact that the largest contribution stems from the interlayers with DDL thicknesses of 1-3 water layers the Debye length multiplier is commonly set to low values, i.e. ≤1 (Alt-Epping et al. 2014; Tournassat & Steefel 2015).

There is a rather fundamental difference how cation exchange is handled in the two model types: In the AFI models the interlayer surface charge is completely screened by exchangeable cations, whereas this is not the case in DS models. In fact, in most simple DS model no screening of the negative surface charge is assumed, and cations are distributed between the free solution and the DDL according Donnan equilibrium. Thus, the concentrations of cations in the Donnan space are governed by charge, but not by chemical constraints. The selectivity of exchangeable cations, can however be considered by partial screening of the surface with surface complexed (immobile) cations (Appelo & Wersin 2007; Appelo et al. 2010; Alt-Epping et al. 2014).

The adequacy of DS model approach for describing anion-accessible porosity data has so far – to the best of our knowledge- not been assessed in a systematic way. However, a few very recent modelling studies have been carried out on experimental diffusion data. Tournassat & Steefel (2015) presented two DS modelling exercises for simulating the experimental data of Tachi & Yotsuji (2014) and of Glaus et al. (2013). In both cases partial screening of the surface charge by cations sorbed in the Stern layer was assumed. The simulated breakthrough behaviour of the anionic (I^-) and other tracers (HTO, $^{22}Na^+$, $^{137}Cs^+$) showed a good match with the experimental data of Tachi & Yotsuji (2014) which involved ionic strength of 0.1 M $NaClO_4$. In the case of the second dataset of Glaus et al. (2013) diffusion of $^{22}Na^+$ under salinity gradient in two diffusion experiments was modelled. An equally good match of the experimental data could be achieved as with the AFI model applied by Glaus et al. (2013).

A benchmark modelling exercise involving different reactive transport simulators was performed by Alt-Epping et al. (2014) on a flow-through column experiment for which an extensive chemical and hydraulic dataset was available (Jenni et al. 2014). Besides more conventional model approaches, a DS model with two porosity domains (Donnan and “free” solution) was applied using PHREEQC (Parkhurst & Appelo 2013) and CrunchFlowMC (Steefel et al. 2014), which are so far the only reactive transport simulators including the electrostatic effects in clays (Tournassat & Steefel 2014). Also, in this DS model, partial screening of the surface charge by sorbed cations was assumed. A central result was that only the DS model could simulate experimental breakthrough curves for major cations and anions adequately.

In summary, the results highlight that multicomponent diffusion models including an electrostatic description of the clay-water interface are required to properly simulate experimental diffusion data. It appears that the two models (AFI and DS) involving two widely different assumptions regarding the treatment of interlayer water adequately describe these experimental data.

2.3 Setting up a geochemical model

As is evident from the discussion in the previous sections, there are considerable uncertainties related to microstructural and electrostatic properties of compacted bentonite in spite of the progress made in the last years. Two cases representing implementations of the two conceptual models described above and which are thought to encompass most of these uncertainties, will be considered: the first is based upon the AFI triple porosity model concept and the second on the DF double porosity concept. The two cases represent bounding cases with regard to the treatment of the montmorillonite surface charge and of cation exchange: in the AFI model the major part of the surface (the internal surface) is screened by sorbing (exchangeable) cations, whereas in the applied DS model the entire surface charge is compensated in the DDL by the cation-enriched solution.

Both cases build on the well-established thermodynamic bentonite models (Wieland et al. 1994; Wersin 2003; Bradbury & Baeyens 2003) developed on the basis of experimental data at low compaction (Wanner et al. 1992; Bradbury & Baeyens 1997; 2002; Muurinen & Lehikoinen 1999). Reactions at the montmorillonite surface include cation exchange and protonation/deprotonation via surface complexation. The montmorillonite is otherwise considered to be inert, which is deemed justified in view of the low solubility of this phase for the geochemical conditions considered (Wersin et al. 2014a). However, the dissolution/precipitation of selected accessory minerals, such as gypsum, calcite, quartz and kaolinite is included in the model.

AFI model:

This model is based on the approach presented in Wersin et al. (2004), but considers the microstructural concept of montmorillonite presented above. The proportion of the porosity types, i.e. IL, DDL and "free" are derived from the "crystallographic" specific montmorillonite surface area (765 m^2/g) and an assumed fixed stacking number of 15 and a Debye length multiplier of 1. The stacking number is an uncertain parameter, depending on a number of poorly constrained factors (see above). The stacking number of 15 is deemed reasonable based on the microscopic observations of Melkior et al. (2009) and moreover such a number leads to fairly high proportion of IL (eq. 4) as opposed to the DS model. The selection of a Debye length multiplier of 1 for the DDL is based on the space considerations (see above) and considerations of Tournassat & Appelo (2011). The diffuse double layer model of Borkovec & Westall (1983) is applied which is implemented in PHREEQC and has been used in previous studies (Curti & Wersin 2002; Wersin 2003; Wersin et al. 2004). The parameters for cation exchange and surface complexation were also selected from those studies and are listed in Table 1.

DS model:

As outlined above, the IL and DDL are considered as a single Donnan space. The distribution of cations and anions in the Donnan space and the "free" water is governed by Donnan equilibrium. It is assumed that the activity ratio between the species concentration in the free and in the DDL is equal to one, as implemented in PHREEQC v.3. A further assumption is that the full negative surface charge is compensated by cations in the Donnan space, hence no screening of the surface charge by complexed cations occurs.

Scoping calculations revealed that, owing to the high surface charge, the Donnan space becomes large at lower ionic strength. Application of eq. (7) at high densities points to Debye lengths smaller than one, thus to overlapping of the DDL. The extent of overlap, however, is difficult to constrain with our model approach. The same feature has previously been noted when the DS was applied to high density clay systems (e.g. Tournassat & Steefel 2015). Because of this difficulty and for better comparison of the two models, we adapt the DDL length such that the proportion of "free" water in the DS model matches that obtained for AFI model. As in the AFI model, the protonation/deprotonation at the external surface is considered. The corresponding parameters are presented in Table 1.

353 *Table 1 Parameters used for geochemical bentonite model. AFI (anion-free interlayer) and DS (Donnan*
354 *space) represent two model variants as discussed in the text.*

	Unit	AFI model	DS model	Comment
Structural parameters				
Specific montmorillon. surface area	m^2/g	765	765	see text
TOT stacking number		15	1	"
DDL length multiplier		1	<1,variable	see text
Montmorillonite mass fraction		0.75	0.75	"
DDL parameters				
Model used for diffuse layer		DDL*	Donnan	DDL*: Borkovec & Westall 1983
Considered porosity		external	int.+ext.	
Cation exchange parameters				
CEC	eq/kg	0.787	0.787	Bradbury & Baeyens 2002
Initial occupancies	equiv. fraction	Na 0.848 Ca 0.084 Mg 0.051 K 0.017		Bradbury & Baeyens 2002
$\log K_{Na/Ca}$		0.41		Gaines-Thomas convention used for cation exchange model
$\log K_{Na/Mg}$		0.31		"
$\log K_{Na/K}$		0.60		"
Surface complexation parameters				
Surface site concentration	eq/kg	0.0284	0.0284	Wieland et al. 1994
Surface area	m^2/g	31.5	31.5	Bradbury & Baeyens 2002
logK: $\equiv SOH + H^+ = \equiv SOH_2^+$		5.4	5.4	Wieland et al. 1994
logK: $\equiv SOH = \equiv SO^- + H^+$		-6.7	-6.7	"
Dissolution of accessories / inventories				
NaCl	mol/kg	1.35E-03	1.35E-03	Bradbury & Baeyens 2002, complete dissolution
Gypsum [1]	mol/kg	0.0235	0.0235	Bradbury & Baeyens 2002
$CaSO_4 \cdot 2H_2O \leftrightarrow Ca^{2+} + SO_4^{2-} + 2H_2O$	logK	-4.61	-4.61	Giffaut et al. 2014
Calcite [1]	wt%	0.7	0.7	Madsen 1998
$CaCO_3 \leftrightarrow Ca^{2+} + CO_3^{2-}$	logK	-8.48	-8.48	Giffaut et al. 2014
Quartz [1]	wt%	10–15	10–15	Madsen 1998
$SiO_2 + 2H_2O \leftrightarrow H_4SiO_4$	logK	-3.74	-3.74	Giffaut et al. 2014
Kaolinite [1]	wt%	Traces	Traces	Madsen 1998
$Al_2Si_2O_5(OH)_4 + 6H^+ \leftrightarrow 2Al^{+3} + H_4SiO_4 + H_2O$	logK	6.51	6.51	Giffaut et al. 2014

355 [1] excess of these minerals assumed in all calculations

356 ## 3. Application to the bentonite buffer at the Olkiluoto site

357 ### 3.1 The bentonite buffer and groundwater chemistry

358 The engineered barrier system (EBS) for spent fuel waste at Olkiluoto is based on the KBS-3 disposal
359 concept (Posiva 2013a): Waste containing copper canisters, surrounded by partially saturated
360 compacted bentonite blocks (buffer), are emplaced in vertical deposition holes (Fig . 3), spaced at 10 m

at about 400 m depth below surface. The deposition holes and the overlying deposition tunnel are surrounded by variably fractured gneissic host rock.

The target density of the buffer is 2.0 kg/dm^3 at full saturation, thus corresponding to a dry density of 1.57 kg/dm^3. The reference buffer material is MX-80 Na-rich bentonite, but alternative bentonites with similar sealing properties are also being considered (Juvankoski et al. 2012). According to the disposal concept, after repository closure, saturation and swelling of the bentonite buffer will proceed via slow groundwater inflow from the host rock. Saturation times are expected to be variable and controlled on the one hand by the rate of water inflow and on the other by coupled thermo-hydro-mechanical behaviour in the buffer which is affected by elevated temperatures in the contacting canister (Posiva 2013a). Thus, saturation times will vary and have been estimated to be in the range of decades to several hundreds of years (Posiva 2013a). Upon saturation, hydromechanical conditions will become more stable, due to the low hydraulic conductivity (~10^{-13}–10^{-14} m/s) and high swelling pressure (6–8 MPa) (Karnland et al. 2006) and slow diffusive transport will dominate.

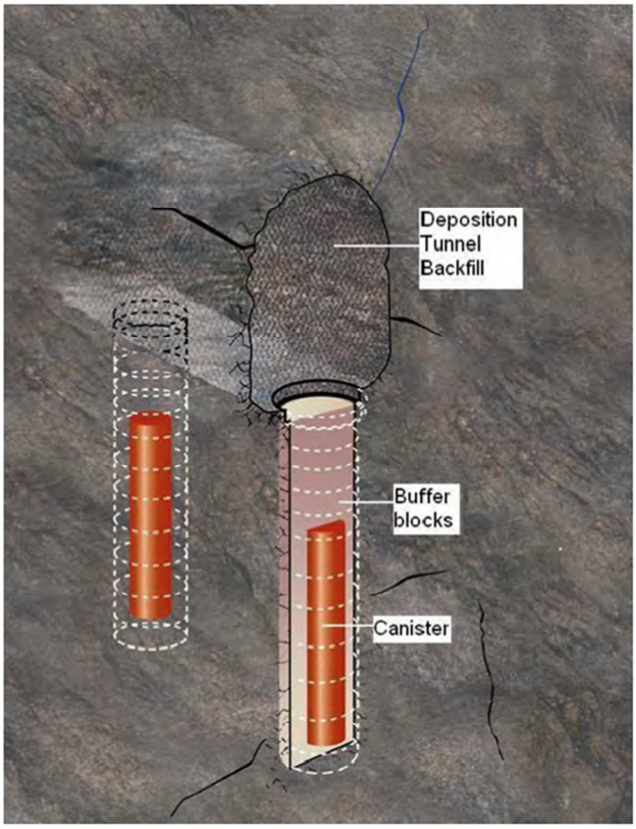

Fig. 3: Schematic view of KBS-3 repository components (Posiva 2012). Of interest here are the bentonite buffer blocks surrounding the canister.

The groundwater composition at repository depth is fairly saline, Na-Cl dominated with a ionic strength of ~0.2 M and total dissolved solids (TDS) of ~10g/L (Table 2). Due to continuing land uplift and climatic changes, the groundwater at repository level is predicted to become more dilute and more influenced by shallower brackish groundwaters with time (Posiva 2013a). Depending on the conditions, it has been envisioned that very dilute groundwaters could reach repository levels during the next glaciation (Posiva 2013a). On the basis of the expected hydrochemical evolution reference groundwaters have been

384 defined (Hellä et al. 2014). These serve to bound the range of groundwater composition in contact with
385 the bentonite buffer. For that purpose, specific groundwater compositions based on samples from deep
386 boreholes were derived, assuming calcite and quartz equilibrium at 25 °C. Table 2 depicts two reference
387 groundwaters in the "groundwater" columns: a saline type, representing present conditions at
388 repository levels and a dilute type representing a bounding groundwater composition.

389 **3.2 Defining initial conditions**

390 The purpose here is to define the initial geochemical conditions in the bentonite buffer (Curti & Wersin
391 2002). Here we assume that in the beginning of the analysis the buffer is fully saturated and that the
392 thermal pulse arising from the decay of short lived nuclides in the waste has dissipated. We consider
393 diffusive equilibration between bentonite porewater and the surrounding groundwater, but also a case
394 is considered in which groundwater is instantaneously admixed with the bentonite buffer.

395 In a first step, the composition of the initial porewater for all cases was defined, following the procedure
396 proposed in Wersin et al. (2004). The initial exchanger composition and accessory minerals (calcite,
397 gypsum, quartz and kaolinite) and the external surface were equilibrated with a solution containing
398 NaCl according to its inventory in the bentonite (Table 1) under a partial pressure of CO_2 (pCO_2)
399 corresponding to atmospheric conditions ($10^{-3.44}$ bar). This resulting surface and porewater composition
400 was then equilibrated with the surrounding groundwater as outlined in the following section.

401 The impact of selecting different initial conditions, such as different pCO_2, different exchanger
402 composition or NaCl concentration, on the results was also tested (section 3.4).

403 *Table 2 Concentrations of selected constituents in groundwater and calculated "free" porewater (pw) in mmol/kg$_w$ for saline and dilute case.*
404 *SI: saturation index; diff. eq.: diffusive equilibration; mixing: mixing assumption (see text).*

	Saline case				**Dilute case**			
	groundwater	**"free" porewater**			**groundwater**	**"free" porewater**		
Model type Constraint		**DS** diff. eq.	**AFI** diff. eq.	**AFI** mixing		**DS** diff. eq.	**AFI** diff. eq.	**AFI** mixing
Ionic strength	215.1	243.2	242.5	454.1	18.9	91.9	94.8	95.5
pH	7.27	7.25	7.27	7.10	7.49	7.15	7.16	7.16
Alkalinity [1]	0.63	0.61	0.63	0.51	4.27	2.32	2.33	2.32
Na	116.1	122.4	131.3	213.9	13.2	33.8	36.1	36.5
K	0.28	0.31	0.32	0.50	0.25	0.70	0.65	0.65
Mg	2.6	3.2	3.4	8.2	0.7	7.4	7.8	7.9
Ca	32.8	42.2	38.8	84.8	1.2	12.8	12.7	12.8
Cl	182.5	182.5	182.5	368.5	9.9	9.9	9.9	11.4
CO_3(tot)	0.66	0.64	0.66	0.53	4.50	2.56	2.58	2.56
SO_4	0.21	15.1	16.3	11.0	1.0	31.5	32.7	32.4
Si	0.17	0.17	0.17	0.16	0.18	0.18	0.18	0.18
log(pCO_2)	-2.86	-2.86	-2.86	-2.86	-2.11	-2.11	-2.11	-2.11
SI calcite	0	0	0	0	0	0	0	0
SI gypsum	-1.88	0	0	0	-1.90	0	0	0
SI quartz	0	0	0	0	0	0	0	0

405 [1] $[Alk] = [HCO_3^-]_T + 2[CO_3^{2-}]_T$ where subscript T refers to the total concentration of HCO_3^- and CO_3^{2-}, respectively

3.3 Definition and implementation of scenarios

The goal of the modelling exercise was to compare the compositions for the different water types (IL, DDL and "free") obtained from the AFI and DS model. The buffer which had been pre-equilibrated according to section 3.3 was diffusively equilibrated separately with saline and a dilute external groundwater. This led to four scenarios to be assessed. In addition, for the AFI model a variant was considered in which the (pre-equilibrated) bentonite buffer was (instantaneously) admixed with saline groundwater (Wersin et al. 2004, Wersin et al. 2014a). With regard to cation exchange, it was further assumed that the exchanger composition in the AFI model is controlled by that of the external "free" porewater. In this way, the results can be readily compared with the DS model, although we are aware that equilibration of the exchanger may take a long time (Neretnieks et al. 2009). The six scenarios assessed are shown in Table 3.

The accessory minerals were assumed to be present excess in the buffer in all calculations. In the case of gypsum, which is fairly soluble, complete dissolution might be expected with time in view of the undersaturated conditions with respect to this phase in the crystalline groundwater. On the basis of hydraulic data and reactive transport modelling, it has been shown (Wersin et al. 2014b), however, that the gypsum is expected to persist for long timescales.

Table 3: Model scenarios for deriving porewater composition of bentonite buffer. Fractions of different porosity types (IL: interlayer; DDL: diffuse double layer, "free") also shown (see text)

Model scenario	Model approach	Contacting groundwater	Assumption for chloride	% IL	%DDL	%"free"
AFI_saline_a	AFI	Saline type	$[Cl]_{free} = [Cl]_{gw}$	61.1	7.7	31.2
AFI_saline_b	AFI	Saline type	Mixing model	61.1	7.7	31.2
AFI_dilute_a	AFI	Dilute type	$[Cl]_{free} = [Cl]_{gw}$	63.1	32.6	4.3
AFI_dilute_b	AFI	Dilute type	Mixing model	63.1	32.6	4.3
DS_saline	DS	Saline type	$[Cl]_{free} = [Cl]_{gw}$	0	78.8	31.2
DS_dilute	DS	Dilute type	$[Cl]_{free} = [Cl]_{gw}$	0	95.7	4.3

AFI: anion-free interlayer; DS: Donnan space

Calculation of porosity distributions:

This calculation of the porosity distribution for the AFI model is straightforward based on the assumptions and the structural model detailed in sections 2.3 and 2.1, respectively. The derived proportions for IL, DDL and "free" water are shown in Table 3. As expected, the proportion of "free" water in the external porespace decreases with decreasing ionic strength, whereas that of the DDL increases. For the DS model, the proportions are derived as outlined in section 2.3.

Implementation in PHREEQC:

Calculations were based on the thermodynamic equilibrium model outlined in section 2.3. The thermodynamic database THERMOCHIMIE Version 9 (Giffaut et al. 2014) was applied and a temperature of 25 °C was assumed throughout which is somewhat above the reference temperature (~12 °C) in the surrounding rock. The reasons for selecting 25 °C for the calculations were: (i) the

minimisation of data uncertainties by using standard state conditions and (ii) the small differences in the results expected from the temperature effect.

The groundwater solution was equilibrated with the pre-equilibrated bentonite considering cation exchange and surface complexation reactions, as well as the dissolution / precipitation of accessory minerals according to the premises outlined in Table 1. For the diffusive equilibration scenarios, the anions concentrations in the "free" porewater were fixed to that in the groundwater by addition of small amounts of NaCl and NaBr.

3.4 Results

The modelled data with the full composition is presented in the Supplementary data (Table SD-1). Table 2 shows selected results for the "free" porewater compositions and compares these with the corresponding groundwater data. A conspicuous feature is the similarity of the AFI and DS model results, which a priori was not expected in view of the very distinct model assumptions with regard to constraints for cations. This holds for the assessment scenarios in which diffusive equilibration between groundwater and porewater is assumed. Changing the initial porewater and exchanger composition (section 3.3.) resulted in only a marginal influence on the final compositions.

The differences between the "free" porewater and groundwater compositions are also fairly small for the assessment scenarios assuming diffusive equilibration. The main difference arises from the gypsum equilibrium in the buffer, leading to higher sulphate and calcium levels in the "free" porewater.

The assumption of instantaneous mixing of groundwater with the bentonite buffer, leads to a higher ionic strength in the saline case because of anion exclusion in the interlayer and the consequent concentration of solutes in the external pores and different composition in the "free" porewater. For the dilute case, however, this concentration effect is largely outcompeted by the large proportion of DDL relative to "free" pore space (Table 4).

The concentrations of the main constituents in the DDL and the composition of exchangeable cations are shown in Table 4 (in mmol per kg DDL water and per kg interlayer water). Obviously, owing to the assumptions inherent in the two models, there are large differences in the cation concentrations in the different compartments. In the AFI model the internal negative surface charge is entirely compensated by exchangeable cations, whereas in the DS model the charge compensation occurs entirely in the diffuse layer (Donnan) space. The proportions of Na, Ca and Mg in the exchange complex in the AFI model and those in DDL in the DS model are slightly different, where the Ca/Na and Mg/Na ratios are higher in the DS model (Table 4; see Discussion section).

Table 4 Concentrations of selected constituents in mmol/kg DDL water and mmol/kg IL water, >S- represents surface complexation sites

	Saline case			Dilute case		
Model Constraint	DS diffusive eq.	AFI diffusive eq.	AFI mixing	DS diffusive eq.	AFI diffusive eq.	AFI mixing
DDL						
% total porosity	68.8%	7.7%	7.7%	95.7%	32.6%	32.6%
Na	778.0	286.8	317.8	322.6	51.0	51.2
K	1.96	0.71	0.75	6.75	0.92	0.93
Mg	118.5	15.4	19.9	515.4	17.1	17.2
Ca	1632.5	178.5	216.6	840.0	26.8	26.9
Cl	39.7	11.4	151.8	1.6	5.0	5.7
C	1.20	0.23	0.35	1.78	1.49	1.49
S	10.6	0.4	5.2	8.0	14.1	14.1
>S-OH	74.5	628.9	654.8	42.8	155.4	153.8
$>S\text{-}O^-$	72.8	692.9	662.1	61.4	113.4	115.3
$>S\text{-}OH_2^+$	3.8	28.6	32.5	42.8	10.7	10.3
Interlayer (IL)						
% total porosity	0%	61.0%	61.0%	0%	63.1%	63.1%
NaX		1995.2	2100.0		1000.2	978.8
CaX_2		1257.7	1208.2		1152.4	1125.3
MgX_2		89.3	86.8		640.7	626.6
KX		19.6	19.7		72.3	70.7

The concentrations of anions (Cl, SO_4) in the diffuse layer are lower compared to the "free" water because of the effect of the negative surface charge. They are also affected by the ionic strength, thus decreased in the dilute case.

3.5 Discussion

Application of "reference porewater" concept:

The derivation of so-called reference porewaters of the bentonite buffer based on thermodynamic modelling is a common approach in safety assessment of high-level waste repositories (Curti & Wersin 2002; Arcos et al. 2006; Bradbury et al. 2014; Wersin et al. 2014a). The compositions of these waters provide the basis for a number of processes considered in safety assessment, such as for example corrosion of the copper canister (Posiva 2013a). They also are used to derive retention parameters for radionuclides, such as solubilities and sorption values. These parameters are subsequently implemented in radionuclide transport calculations with simple diffusion models (Altmann 2008; SKB 2010; Posiva 2013b). The diffusion of radionuclides through the bentonite buffer is particularly affected by pH and complexing ligands such as carbonate and, to lesser extent, sulphate and chloride (Tachi et al. 2014, Wersin et al. 2014a). Thus, the robustness of the geochemical model and the uncertainties of the derived porewater composition play an important role in safety assessment. The results presented here suggest that uncertainties related to the electrostatic properties and description of different porosities of the bentonite do not have a large effect on the porewater chemistry. Notably, two largely different descriptions of the interlayer and diffuse double layer yield very similar results in the "free" porewater composition. This can be explained by the large chemical buffering capacity of the bentonite buffer, owing to its large cation

494 and proton exchange capacity and the presence of reactive accessory minerals, such as gypsum and
495 calcite.

496 Larger differences arise when equilibration between the porewater and surrounding groundwater is
497 based on the mixing assumption rather than by diffusive equilibration (see above). The mixing
498 assumption (i.e. instantaneous admixing of the groundwater with the bentonite buffer material) may
499 be appropriate for approximating transient conditions, such as during buffer saturation (Sena et al.
500 2010, Jenni et al. 2014). For longer time periods, the assumption of diffusive equilibration is
501 considered to be more appropriate (Posiva 2013b). From a safety assessment viewpoint, the
502 differences between these two model scenarios are not very relevant with regard to the mobility of
503 radionuclides in the buffer. This is indicated by the fairly similar solubilities and sorption values of RN
504 derived for reference porewaters with the diffusive equilibration and the mixing assumption,
505 respectively (Wersin et al. 2014a).

506 Basis for multicomponent diffusion modelling:

507 As outlined in section 2.2, multicomponent diffusion through compacted bentonite has been
508 successfully described by the AFI and DS model approaches. Also for this reason, the derivation of
509 porewater compositions presented above is based upon these approaches. The proportions in the
510 "free", DDL and interlayer normalised per volume of total water illustrate the predominance of the
511 cation load in the interlayer (AFI model) and Donnan space (DS model), respectively (Fig. 4). This
512 reflects the large difference with regard to surface charge shielding inherent in the two approaches
513 (see above). It should be noted that in the DS model there is the possibility to shield a part of the
514 surface charge by fixing cations in the Stern layer (Tournassat & Steefel 2015) and thus diminishing
515 the cation load in the Donnan layer. The attributed fractions of cations in these two layers seem,
516 however, to be an arbitrary choice in view of the lack of theoretical or experimental basis (Alt-Epping
517 et al. 2014; Tournassat & Appelo 2015).

518 The effect of anion exclusion is mirrored by the chloride concentrations in the different porosities
519 (Fig. 4). In the saline case, the main chloride load predicted by the AFI model is in the "free" porosity
520 and only a minor fraction occurs in the diffuse layer. The DS model, on the other hand, predicts
521 similar chloride loads in both porosity spaces. In other words, the DS model predicts somewhat
522 higher Cl^- concentrations and thus also higher diffusive fluxes in the DS model relative to the AFI
523 model. In the dilute case, both models yield fairly similar results and higher Cl^- loads in the diffuse
524 layer compared to the "free" porosity space.

525 The different approaches used for describing the DDL in the AFI and DS models, i.e. the Gouy-
526 Chapman based model of Borkovec & Westall (1983) and the Donnan approximation, respectively,
527 yield very similar results in terms of composition in the DDL (not shown). This is because both
528 approaches are based on similar equations, as shown for example in Tournassat & Steefel (2015).

529

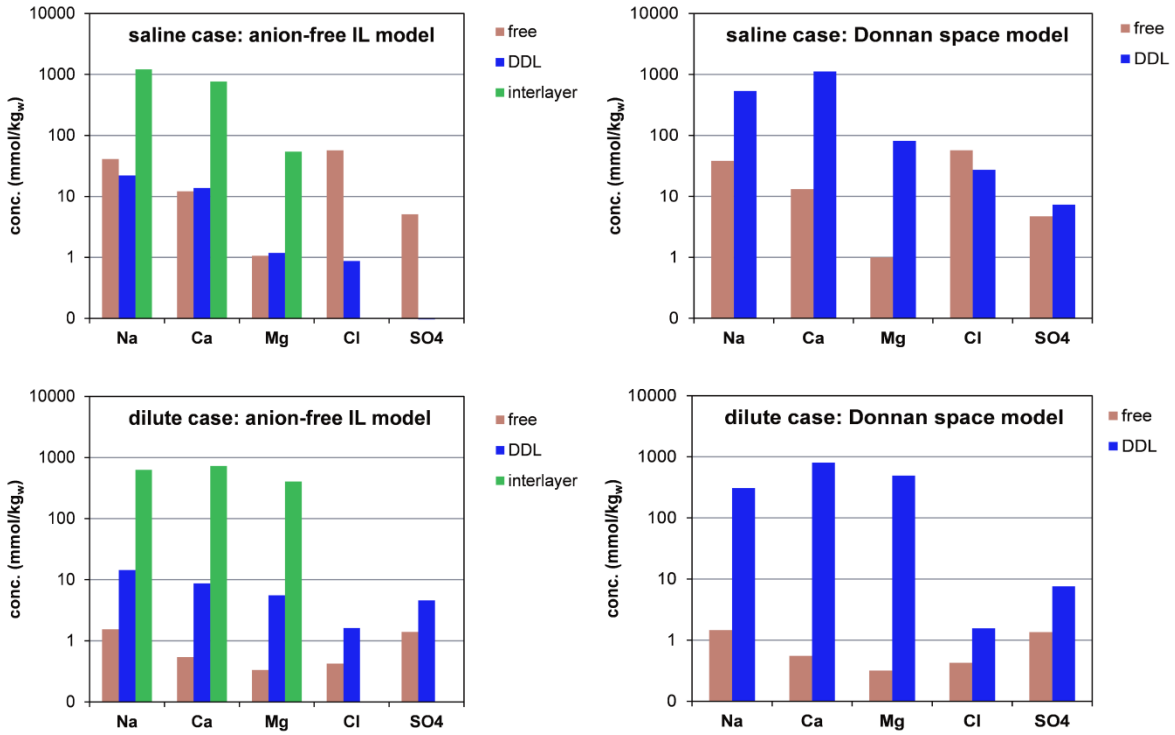

Fig. 4: Concentrations (mmol/kg of total water) of selected constituents in different porosity compartments: upper: saline case; lower: dilute case

Conceptual issues:

In view of the considerable uncertainty regarding the porewater chemistry in the interlayer two distinct model descriptions (anion-free, Donnan space) have been applied. In the Donnan space model, the activity coefficients of species in the diffuse layer are commonly assumed to be the same as in the "free" porewater (Appelo et al. 2010; Steefel et al. 2014). This assumption is questionable, in particular for cations whose concentrations are in molar range. Activities may be affected by the high surface charge (Tournassat & Appelo 2015), ion pair formation (Charlet & Tournassat 2005; Bourg & Sposito 2011) and the decreased dielectric constant of water (Teschke et al. 2001). The activity of divalent cations Ca^{2+} and Mg^{2+} is expected to be more influenced than that of Na^{+} (Ferrage et al. 2005), thus diminishing their selectivity in the diffuse layer.

Diffusive equilibration between the external groundwater and the buffer porewater is deemed to be reasonable assumption when long timescales are considered. The time scale for diffusive mixing was estimated from diffusion calculations to be a few hundreds to a few thousands of years (Wersin et al. 2014b) whereas the period for evaluating repository safety comprises 10^5 to 10^6 years.

During transient conditions, the choice of model and the treatment of interlayer water will affect the evolution of porewater chemistry and the time when equilibrium will be reached, as indicated by the different chloride inventories (see above). This will be assessed in a subsequent contribution (Wersin et al., in prep.).

On a more general level, the estimation of the different porosity fractions is based upon simplified crystallographic and geometrical considerations neglecting the heterogeneous micro/nano structure. Thus, layer collapse or the presence of gel-type domains (Tournassat & Appelo 2011,

Pusch 2001; Keller et al. 2014). With regard to the porewater chemistry, such features are not expected to lead to strong effects. The two models representing widely different descriptions of the porosity are thought to represent bounding cases encompassing the different structural configurations.

4. Conclusions

A structural model based upon simple crystallographic and electrostatic principles has been set up to derive the different porosity types in compacted bentonite. In view of the uncertainty related to the chemical properties of the interlayer water two differing model concepts (anion-free interlayer, Donnan space) together with a well-established thermodynamic model for bentonite were applied to derive the porewater composition of the bentonite buffer for the Finnish nuclear repository site. The simulations indicate very similar results in the "free" water composition for the two models under the assumption of diffusive equilibration between the porewater and the surrounding groundwater of the host rock. This result supports the validity of the reference porewater concept in safety assessment as basis for deriving radionuclide solubility and sorption parameters. It also indicates that the conceptual model uncertainties related to the microstructure of compacted bentonite have a minor effect on its "free" porewater composition.

Due to the different assumptions inherent in the two models larger differences arise in the simulated composition of the water affected by the negative surface charge. This is expected to have consequences in the modelling of the transient porewater chemistry evolution. Further experimental evidence is required to decide which type of multi porosity diffusion model is more appropriate for describing this transient evolution.

Acknowledgements

Part of this work has been carried within Posiva's TURVA-2012 project and has benefitted from the assistance of Tony Appelo (Amsterdam) and Dominic Rosch (Gruner Ltd). We also express our thanks to Margit Snellman (Saanio & Riekkola), Christoph Tournassat (BRGM), Andreas Jenni, Thomas Gimmi and Peter Alt-Epping (University of Bern) for fruitful discussions. The paper has significantly benefitted from the comments of two anonymous reviewers. Partial funding by Posiva Oy is acknowledged.

5. References

Alt-Epping, P., Tournassat, C., Rasouli P., Steefel, C.I., Mayer, K.U., Jenni, A., Mäder, U., Sengor, S.S., Fernández, R., 2014. Benchmark reactive transport simulations of a column experiment in compacted bentonite with multispecies diffusion and explicit treatment of electrostatic effects. Comput. Geosci., DOI 10.1007/s10596-014-9451-x.

Altmann, S., 2008. 'Geo'chemical research: A key building block for nuclear waste disposal safety cases. J. Contam. Hydrol. 102, 174-179.

Andra, 2005. Dossier 2005 Argile: Safety evaluation of a geological repository, Châtenay-Malabry, France.

Appelo, C.A.J., 2013. A review of porosity and diffusion in bentonite. Posiva Working Report WR-2013-29, Posiva Oy, Eurajoki, Finland. http://www.posiva.fi/en/databank/working_reports/.

Appelo, C.A.J., Wersin, P., 2007. Multicomponent diffusion modeling in clay systems with application to the diffusion of tritium, iodide and sodium in Opalinus Clay. Environ. Sci. Technol. 41, 5002-5007.

Appelo, C.A.J., Van Loon, L.R., Wersin, P., 2010. Multicomponent diffusion of a suite of tracers (HTO, Cl, Br, I, Na, Sr, Cs) in a single sample of Opalinus Clay. Geochim. Cosmochim. Acta 74, 1201-1219.

Arcos, D., Grandia, F., Domenech, C., 2006. Geochemical evolution of the near field of a KBS-3 repository. SKB Technical Report TR-06-16, Stockholm Sweden. http://www.skb.com/publications/.

Baeyens, B., Bradbury, M.H., 1997. A mechanistic description of Ni and Zn sorption on Na-montmorillonite. Part I: Titration and sorption measurements. J. Contam. Hydrol. 27, 199-222.

Birgersson, M., Karnland, O., 2009. Ion equilibrium between montmorillonite interlayer space and an external solution —Consequences for diffusional transport. Geochim. Cosmochim. Acta 73, 1908-1923.

Borkovec, M., Westall, J. 1983., Solution of the Poisson-Boltzmann equation for surface excesses of ions in the diffuse layer at the oxide-electrolyte interface. J. Electroanal. Chem. 150, 325-337.

Bourg, I.C., Sposito, G., 2011. Molecular dynamics simulations of the electrical double layer on smectite surfaces contacting concentrated mixed electrolyte ($NaCl–CaCl_2$) solutions. J. Colloid Interf. Sci. 360, 701-715.

Bourg, I.C., Sposito, G., Bourg, A.C.M., 2006. Tracer diffusion in compacted, water-saturated bentonite. Clays Clay Min. 54, 363-374.

Bradbury, M.H., Baeyens, B., 1997. A mechanistic description of Ni and Zn sorption on Na-montmorillonite. Part II. Modelling. J. Contam. Hydrol. 27, 223-248.

Bradbury, M.H., Baeyens, B., 2002. Porewater chemistry in compacted re-saturated MX-80 bentonite: physico-chemical characterisation and geochemical modelling. Nagra Technical Report NTB 01-08, Wettingen, Switzerland. http://www.nagra.ch/en/cat/publikationen/technicalreports-ntbs/ntbs-2001-2013/downloadcentre.htm.

Bradbury, M.H., Baeyens, B., 2003. Porewater chemistry in compacted re-saturated MX-80 bentonite. J. Contam. Hydrol. 61, 329-338.

Bradbury, M.H., Berner, U., Curti, E., Hummel, W., Kosakowski, G., Thoenen, T., 2014. Evolution of the near-field of a HLW repository. Nagra Technical Report NTB 12-01, Wettingen, Switzerland. http://www.nagra.ch/en/cat/publikationen/technicalreports-ntbs/ntbs-2001-2013/downloadcentre.htm.

Bruno, J., Arcos, D., Duro, L., 1999. Processes and features affecting the near field hydrochemistry. Groundwater - bentonite interactions. SKB Technical Report TR-99-29, Stockholm, Sweden. http://www.skb.com/publications/.

Charlet, L., Tournassat, C., 2005. Fe(II)-Na(I)-Ca(II) cation exchange on montmorillonite in chloride medium : evidence for preferential clay adsorption of ions pairs in marine environment chemical modelling and XRD profile modelling study. Aquat. Geochem. 11, 115-137.

Cuevas, J., Villar, M.V., Fernández, P., Gómez, P., Martín, P.L., 1997. Pore waters extracted from compacted bentonite subjected to simultaneous heating and hydration. Appl. Geochem. 12, 473-481.

Curti, E., Wersin, P., 2002. Assessment of porewater chemistry in the bentonite backfill for the Swiss SF/HLW repository. Nagra Technical Report NTB 02-09, Wettingen, Switzerland.

http://www.nagra.ch/en/cat/publikationen/technicalreports-ntbs/ntbs-2001-2013/downloadcentre.htm.

Ferrage, E., Tournassat, C., Rinnert, E., Charlet, L., Lanson, B., 2005. Experimental evidence for calcium-chloride ion pairs in the interlayer of montmorillonite. A XRD profile modeling approach. Clays Clay Miner. 53, 348-360.

Giffaut, E., Grivé, M., Blanc, P., Vieillard, P., Colàs, E., Gailhanou, H., Gaboreau, S., Marty, N., Madé, B., Duro, L. 2014. ANDRA thermodynamic database for performance assessment: ThermoChimie. Appl. Geochem. 49, 225–236.

Glaus, M.A., Frick, S., Rossé, R., Van Loon, L.R., 2010. Comparative study of tracer diffusion of HTO, $^{22}Na^{+}$ and $^{36}Cl^{-}$ in compacted kaolinite, illite and montmorillonite. Geochim. Cosmochim. Acta 74, 1999-2010.

Glaus, M.A., Birgersson, M., Karnland, O., Van Loon, L.R., 2013. Seeming steady-state uphill Diffusion of $^{22}Na^{+}$ in compacted montmorillonite. Environ. Sci. & Technol. 47, 11522-11527.

Hellä, P., Pitkänen, P., Löfman, J., Partamies, S., Vuorinen, U., Wersin, P., 2014. Safety case for the disposal of spent nuclear fuel at Olkiluoto. Definition of reference and bounding groundwaters, buffer and backfill porewaters. Report Posiva 2014-04, Posiva Oy, Eurajoki, Finland. http://www.posiva.fi/en/databank/posiva_reports/.

Jenni, A., Mäder, U., Fernández, R., 2014. Multi-component advective-diffusive transport experiment in MX-80 compacted bentonite: Method and results of 2nd phase of experiment and post mortem analysis. Nagra Arbeitsbericht NAB 14-22, Nagra, Wettingen, Switzerland.

Juvankoski, M., Ikonen, K., Jalonen, T. 2012. Buffer Production Line 2012. Design, production and initial state of the buffer. Report POSIVA 2012-17, Posiva Oy, Eurajoki, Finland. http://www.posiva.fi/en/databank/posiva_reports/.

Karnland, O., Olsson, S., Nilsson, U., 2006. Mineralogy and sealing properties of various bentonites and smectite-rich clay materials. SKB Technical Report TR-06-30, Stockholm, Sweden. http://www.skb.com/publications/.

Keller, L.M., Seiphoori, A., Gasser, P., Falk, L., Holzer, L., Ferrari, A., 2014. The pore structure of compacted and partly saturated MX-80 bentonite at different dry densities. Clays Clay Miner. 62, 357-372.

Kiviranta, L., Kumpulainen, S., 2011. Quality control and characterization of bentonite materials. Posiva Working Report 2011-84, Posiva Oy, Eurajoki, Finland. http://www.posiva.fi/en/databank/working_reports/.

Kozaki, T., Saito, N., Fujishima, A., Sato, S., Ohashi, H., 1998. Activation energy for diffusion of chloride ions in compacted montmorillonite. J. Contaminant Hydrology 35, 67-75.

Kozaki, T., Inada, K., Sato, S., Ohashi, H., 2001. Diffusion mechanism of chloride ions in sodium montmorillonite. J. Contam. Hydrol. 47, 159-170.

Kozaki, T., Liu, J., Sato, S., 2008. Diffusion mechanism of sodium ions in compacted montmorillonite under different NaCl concentration. Phys. Chem. Earth 33, 957-961.

Le Forestier, L., Muller, F., Villieras, F., Pelletier, M., 2010. Textural and hydration properties of a synthetic montmorillonite compared with a natural Na-exchanged clay analogue. Appl. Clay Sci. 48, 18–25.

Leroy, P., Revil, A., Coelho, D., 2006. Diffusion of ionic species in bentonite. J. Colloid Interf. Sci. 296, 248-255.

Madsen, F.T., 1998. Clay mineralogical investigations related to nuclear waste disposal. Clay Miner. 33, 109-129.

Melkior, T., Gaucher, E.B., Brouard, C., Yahiaoui, S., Thoby, D., Clinard, Ch., Ferrage, E., Guyonnet, D., Tournassat, C., Coelho, D., 2009. Na^+ and HTO diffusion in compacted bentonite: Effect of surface chemistry and related texture. J. Hydrol. 370, 9-20.

Molera, M., Eriksen, T., Jansson, M., 2003. Anion diffusion pathways in bentonite clay compacted to different dry densities. Appl. Clay Sci. 23, 69-76.

Muurinen, A., 2006. Ion concentration caused by an external solution into the porewater of compacted bentonite. Posiva Working Report 2006-09, Posiva Oy, Eurajoki, Finland. http://www.posiva.fi/en/databank/working_reports/.

Muurinen, A., Lehikonen, J., 1999. Porewater chemistry in compacted bentonite. Engineer. Geol. 54, 207-214.

Muurinen, A., Penttilä-Hilthunen, P., Uusheimo, K., 1987. Diffusion of chloride and uranium in compacted sodium bentonite. In Scientific basis for nuclear waste management XII (eds. W. Lutze and R. C. Ewing) Mater. Res. Soc. Symp. Proc. Materials Research Society, Pittsburgh, PA.

Muurinen, A., Karnland, O., Lehikoinen, J., 2004. Ion concentration caused by an external solution into porewater of compacted bentonite. Phys. Chem. Earth 29, 119-127.

Muurinen, A., Karnland, O., Lehikoinen, J., 2007. Effect of homogenization on the microstructure and exclusion of chloride in compacted bentonite. Phys. Chem. Earth 32, 485-490.

Nagra, 2002. Project Opalinus Clay: Safety report. Demonstration of disposal feasibility for spent fuel, vitrified high-level waste and long-lived intermediate-level waste (Entsorgungsnachweis). Nagra Technical Report NTB 02-05, Wettingen, Switzerland. http://www.nagra.ch/en/cat/publikationen/technicalreports-ntbs/ntbs-2001-2013/downloadcentre.htm.

Neretnieks, I., Liu, L., Moreno, L., 2009. Mechanisms and models for bentonite erosion. SKB Technical Report TR-09-35, Stockholm, Sweden. http://www.skb.com/publications/.

Ochs, M., Lothenbach, B., Shibata, M., Yui, M., 2004. Thermodynamic modeling and sensitivity analysis of porewater chemistry in compacted bentonite. Phys. Chem. Earth 29, 129-136.

Ohe, T., Tsukamoto, M., 1997. Geochemical properties of bentonite porewater in high-level waste repository condition. Nucl. Technol. 118, 49-57.

Parkhurst, D.L., Appelo, C.A.J., 2013. Description of input and examples for PHREEQC version 3: a computer program for speciation, batch-reaction, one-dimensional transport, and inverse geochemical calculations. No. 6-A43. US Geological Survey.

Plaschke, M., Schäfer, T., Bundschuh, T., Ngo Manh, T., Knopp, R., Geckeis, H., Kim J.I., 2001. Size characterization of bentonite colloids by different methods. Anal. Chem. 73, 4338-4347.

Posiva, 2012. Buffer Production Line 2012 - Design, production and initial state of the buffer. Report Posiva 2012-17, Posiva Oy, Eurajoki, Finland. http://www.posiva.fi/en/databank/posiva_reports/.

Posiva, 2013a. Safety case for the disposal of spent nuclear fuel at Olkiluoto. Performance assessment 2012. Report Posiva 2012-04, Posiva Oy, Eurajoki, Finland. http://www.posiva.fi/en/databank/posiva_reports/.

Posiva, 2013b. Safety case for the disposal of spent nuclear fuel at Olkiluoto. Models and data for the repository system 2012. Report Posiva 2013-01, Posiva Oy, Eurajoki, Finland. http://www.posiva.fi/en/databank/posiva_reports/.

Pusch, R., 2001. The microstructure of MX-80 clay with respect to its bulk physical properties under different environmental conditions. SKB Technical Report TR-01-08, Stockholm, Sweden. http://www.skb.com/publications/.

Rotenberg, B., Marry, V., Vuilleumier, R., Malikova, N., Simon, C., Turq, P., 2007. Water and ions in clays: Unraveling the interlayer/micropore exchange using molecular dynamics. Geochim. Cosmochim. Acta 71, 5089–5101.

Sacchi, E., Michelot, J.-L., Pitsch, H., 2000. Porewater extraction from argillaceous rocks for geochemical characterisation. Nuclear Energy Agency, OECD, Paris.

Sena, C., Salas, J., Arcos, D., 2010. Thermo-hydro-geochemical modelling of the bentonite buffer. SKB Technical Report TR-10-65, Stockholm, Sweden. http://www.skb.com/publications/.

SKB, 2010. Radionuclide transport report for the safety assessment SR-Site. SKB Technical Report TR-10-50, Stockholm, Sweden. http://www.skb.com/publications/.

SKB (2011): Long-term safety for the final repository for spent nuclear fuel at Forsmark. SKB Technical Report TR-11-01, Stockholm, Sweden.

Snellman M., Uotila H., Rantanen J. (1987): Laboratory and modelling studies of sodium bentonite groundwater interaction. Mat. Res. Soc. Symp. Proc. 84, 781-790.

Steefel C.I., Appelo C. A. J., Arora B., Jacques D., Kalbacher · T., Kolditz O., Lagneau V., Lichtner P.C., Mayer K.U., Meeussen J.C.L., Molins S., Moulton D., Shao H., Simunek J., Spycher N., Yabusaki S.B., Yeh G.T. (2014): Reactive transport codes for subsurface environmental simulation. Comput. Geosci. DOI 10.1007/s10596-014-9443-x.

Tachi, Y., Yotsuji, K., 2014. Diffusion and sorption of Cs^+, Na^+, I^- and HTO in compacted sodium montmorillonite as a function of porewater salinity: Integrated sorption and diffusion model. Geochim. Cosmochim. Acta 132, 75-93.

Tachi, Y., Yotsuji, K., Suyama, T., Ochs, M., 2014. Integrated sorption and diffusion model for bentonite. Part 2: porewater chemistry, sorption and diffusion modeling in compacted systems. J. Nucl. Sci. Technol. 51, 1191-1204.

Teschke, O., Ceotto, G., De Souza, E.F., 2001. Interfacial water dielectric-permittivity-profile measurements using atomic force microscopy. Phys. Rev. E 64, 011605.

Tournassat, C., Appelo, C.A.J., 2011. Modelling approaches for anion-exclusion in compacted Na-bentonite. Geochim. Cosmochim. Acta 75, 3698-3710.

Tournassat, C., Steefel, C.I., 2015. Ionic transport in nano-porous clays with consideration of electrostatic effects. Rev. Miner. Geochem. 80, 287-329.

Tournassat, C., Neaman, A., Villiéras, F., Bosbach, D., Charlet, L., 2003. Nanomorphology of montmorillonite particles: Estimation of the clay edge sorption site density by low-pressure gas adsorption and AFM observations. Am. Miner. 88, 1989-1995.

Tournassat, C., Grangeon, S., Leroy, P., Giffaut, E., 2013. Modeling specific pH dependent sorption of divalent metals on montmorillonite surfaces. A review of pitfalls, recent achievements and current challenges. Am. J. Sci. 313, 395–451.

Van Loon, L.R., Glaus, M.A., Müller, W., 2007. Anion exclusion effects in compacted bentonites: Towards a better understanding of anion diffusion. Appl. Geochem. 22, 2356-2552.

Wanner, H., Albinsson, Y., Karnland, O., Wieland, E., Wersin, P., Charlet, L. 1994. The acid/base chemistry of montmorillonite. Radiochim. Acta 66/67, 157-162.

Wersin, P., 2003. Geochemical modelling of bentonite porewater in high-level waste repositories. J. Contam. Hydrol. 61, 405-422.

Wersin, P., Curti, E., Appelo, C.A.J., 2004. Modelling bentonite-water interactions at high solid/liquid ratios: swelling and diffuse double layer effects. Appl. Clay Sci. 26, 249-257.

Wersin, P., Kiczka, M., Rosch, D., 2014a. Safety case for a spent nuclear fuel repository at Olkiluoto. Radionuclide solubility limits and migration parameters for the canister and the buffer. Report

774 Posiva 2012-39, Posiva Oy, Eurajoki, Finland.
775 http://www.posiva.fi/en/databank/posiva_reports/.

776 Wersin, P., Pitkänen, P., Alt-Epping, P., Román-Ross, G., Smith, P., Snellman, M., Trinchero, P.,
777 Molinero, J., Filby, A., Kiczka, M., 2014b. Sulphide fluxes and concentrations in the spent nuclear
778 fuel repository at Olkiluoto. Report Posiva 2014-01, Posiva Oy, Eurajoki, Finland.
779 http://www.posiva.fi/en/databank/posiva_reports/.

780 Wieland, E., Wanner, H., Albinsson, Y., Wersin, P., Karnland, O., 1994. A surface chemical model of
781 the bentonite-water interface and its implications for modelling the near field chemistry in a
782 repository for spent fuel. SKB Technical Report TR 94-26, Stockholm, Sweden.
783 http://www.skb.com/publications/.

Highlights

- The porewater chemistry in bentonite was constrained by geochemical modelling
- Two very different interlayer model concepts yielded similar porewater compositions
- The results indicate the validity of the widely used reference porewater concept
- Differences between the models are evident in the diffuse double layer composition